

## INVESTIGATION OF HEAT TRANSFER AND PRESSURE DROP IN FLEXIBLE METAL HOSES WITH CORRUGATED SURFACES

by

**Sebiha YILDIZ<sup>a\*</sup>, Zeynep Merve ALPARSLAN<sup>b</sup>,  
Ilker COSAR<sup>b</sup>, Salih YAVUZ<sup>b</sup>, Hasan GUNES<sup>c</sup>**

<sup>a</sup>Department of Mechanical Engineering, Yildiz Technical University, Istanbul, Turkiye

<sup>b</sup>Department of Research and Development, Ayvaz Company, Hadımkoy, Istanbul, Turkiye

<sup>c</sup>Department of Mechanical Engineering, Istanbul Technical University,  
Istanbul, Turkiye

Original scientific paper

<https://doi.org/10.2298/TSCI231217154Y>

*In this study, we conducted a numerical investigation of heat transfer and pressure drop in annular corrugated and 1-, 2-, and 3-start spiral-corrugated flexible metal hoses. To validate the numerical results for pressure drop, we established an experimental set-up. The pressure drop results were verified through experimental data, while the numerical heat transfer results were validated against existing correlations in the literature. The results obtained using the corrugated flexible metal hoses were compared to those of a smooth tube, and all hoses along with the smooth tube were 1 meter long. The hydraulic diameters of the annular corrugated hose and the spiral corrugated hoses were 25 mm and 26.2 mm, respectively, with a corrugation depth of 3.2 mm for all hoses. Water, at an average temperature of 25 °C, was used as the fluid, with a constant surface temperature of 70 °C for the test tube. Analyses were conducted for Reynolds numbers ranging from 10000-50000. The results indicated that the fluid outlet temperature and pressure drop values for the annular corrugated hose were generally higher than those for the spiral corrugated hoses. Among the hoses tested, the 1-start spiral corrugated hose showed the highest friction factor, 7.83 times higher than that of the smooth tube. The 3-start spiral corrugated hose achieved the highest Nusselt number, 1.4 times higher than that of the smooth tube, at a Reynolds number of 20000. The performance evaluation criteria for all hoses ranged from 0.6-1.*

Key words: *corrugated flexible metal hoses, turbulent flow, pressure drop, heat transfer, CFD*

### Introduction

Flexible metal hoses are widely utilized in heating, cooling, air conditioning systems, natural gas systems, boiler connections, and chemical and petrochemical plants. These hoses are available in both annular and spiral corrugations, offering pressure resistance, flexibility, and ease of installation. Research has shown that spiral corrugated tubes act as turbulators and vortex generators, disrupting thermal and velocity boundary-layers and causing a well-mixed flow in both laminar and turbulent regions [1, 2]. Several studies have explored spiral corrugated tubes with various designs [1-16]. Kongkaiptaiboon *et al.* [1] conducted numerical simulations to investigate heat transfer, pressure loss, and thermal enhancement factors for air-flowing through spiral corrugated tubes, varying Reynolds numbers, spiral start numbers

\* Corresponding author, e-mail: [syildiz@yildiz.edu.tr](mailto:syildiz@yildiz.edu.tr)

(2-5), and depth ratios ( $d = 50$  mm,  $e/d = 0.02-0.16$ ). Kareem *et al.* [2] numerically studied the heat transfer and pressure drop in a 2-start spiral corrugated tube, analyzing the effects of corrugation parameters  $e/d$  and  $p/d$ . They reported a thermal performance value in the range of 1.8-2.3. Sethumadhavan and Raja Rao [3] examined five spiral corrugated tubes with 1 and 4 corrugation starts, finding a 15-100% increase in tube-side heat transfer coefficient and a 30-200% increase in the friction factors during turbulent flow with water and 50% glycerol compared to that of a smooth tube. Haervig *et al.* [4] conducted a numerical study at  $Re = 10000$  investigating heat transfer in spiral sinusoidal tubes with corrugation heights  $e/d$  and distance between corrugations  $p/d$  ranging from 0-0.16 and 0-2.0, respectively. Promthaisong *et al.* [5] conducted a numerical analysis of the turbulent flow and heat transfer of air in spiral corrugated tubes. They found that spiral corrugated tubes induced vortex flow, enhanced fluid mixing, and contributed to increased heat transfer. Compared to smooth tubes, spiral corrugated tubes led to approximately 0.75-2.35 times higher heat transfer and 1.0-24 times higher pressure drop, achieving a maximum thermal performance factor of 1.16. Pethkool *et al.* [6] experimentally investigated the thermal performance, heat transfer, and friction factor of a helical corrugated tube using water. They tested nine tubes with different pitch/diameter ratios ( $p/d = 0.18, 0.22, 0.27$ ) and corrugation height/diameter ratios ( $e/d = 0.02, 0.04, 0.06$ ), finding a maximum thermal performance factor value of 2.33. Vicente *et al.* [7] studied heat transfer and friction factor using water and ethylene glycol in corrugated tubes within the  $Re = 2000-90000$  range, noting increases of up to 300% in friction factor and 250% in Nusselt number. Dong *et al.* [8] found that corrugated tubes increased heat transfer by 30%-120% and friction factor by 60%-160% in turbulent flows of water and oil compared to smooth tubes. Qian *et al.* [9] analyzed the thermo-hydraulic performance of spiral corrugated tubes with water using numerical simulations. Their study, involving tubes with inner diameters of 10.7 mm and start numbers 2-6 and 8 within the  $Re = 10000-40000$  range, showed performance evaluation criteria (PEC) values from 0.77-1.28, with the highest PEC in the 8-start spiral tube. In their numerical study, Jin *et al.* [10] compared corrugated tubes to smooth tubes focusing on the effects of geometric parameters, fluid properties, and Reynolds numbers, finding friction coefficient increases from 1.9-17.9 and heat transfer coefficient increases from 1.9-9.6. Also, Mimura and Isozaki [11] experimentally studied the effect of corrugated tube geometries on heat transfer and pressure drop using water. Al-Obaidi [12] simulated pressure drop and heat transfer in corrugated tubes with various geometries and validated their results with available experimental data. In another study [13], they investigated heat transfer and fluid-flow in circular pipes with different axial groove numbers, including 2-4, and with different axial groove geometrical configurations under different conditions. Djordjevic *et al.* [14] experimentally investigated the isothermal pressure drop for a steady Newtonian fluid-flow in an Archimedean spiral tube with crosswise corrugations. Ponnusamy *et al.* [15] explored the effects of different types of grooved tubes on heat transfer and friction factor characteristics under turbulent flow. Al-dabagh *et al.* [16] investigated heat transfer, friction factor, and PEC of corrugated tubes with different corrugation depths experimentally and numerically using air as working fluid. The Nusselt number increased up to 105%, and the friction factors were 90-500% higher than those of the smooth tube. Zhai *et al.* [17] carried out a numerical analysis of heat transfer in the range of  $Re = 4000-12000$  using water as the working fluid. They used an annular concave-convex corrugated pipe with a corrugation height of 1-2 mm, corrugation width of 1-2 mm, and  $d = 10$  mm. The Nusselt number decreased as the corrugation height increased. The maximum Nusselt number and the maximum performance factor were 39.8% and 0.9, respectively, compared to those of the smooth tube at the corrugation height of 1 mm.

In the light of the literature so far, the advantages of corrugated tubes for heat transfer have been well-documented through both experimental and numerical data. The literature suggests that corrugations create secondary vortices near the surface of these tubes and cause the flow to mix better than it does in smooth tubes, and thus improving thermal performance. However, the impact of geometry and flow parameters on heat transfer and pressure drop remains complex, which is a gap to be studied further. This study aims to address this gap by investigating how geometric and flow conditions in corrugated tubes affect heat transfer and pressure drop. Previous studies have typically focused on a single type of corrugation with varying geometrical parameters. Here, we compare annular and spiral corrugated flexible metal hoses with different geometrical parameters. This study evaluates whether spiral corrugated hoses offer significantly higher thermal performance and reduced pressure drop compared to the commonly used annular corrugated boiler hoses, given that spiral corrugated hoses are easier to manufacture. The pressure drop and heat transfer of 1-, 2-, and 3-start spiral corrugated hoses, all with the same heat transfer area and corrugation depth ( $e = 3.2$  mm) as the annular corrugated hose, were compared to those of the annular corrugated hose. Experimental pressure drop results under adiabatic conditions were compared with numerical results under the same conditions, while the numerical heat transfer results were validated against existing correlations in the literature.

### Geometric parameters of the flexible metal hoses

We analyzed heat transfer and pressure drop in a smooth tube, annular corrugated hose, and 1-, 2-, and 3-start spiral corrugated hoses. Table 1 presents the geometrical parameters of the 1-start spiral hose, including diameter,  $d$ , corrugation pitch,  $p$ , and depth,  $e$ , along with cross-sectional views of each hose are shown in this table. The geometric parameters for all the flexible metal hose are given in tab. 2.

**Table 1. Schematic representation and cross-section views of the flexible metal hoses**

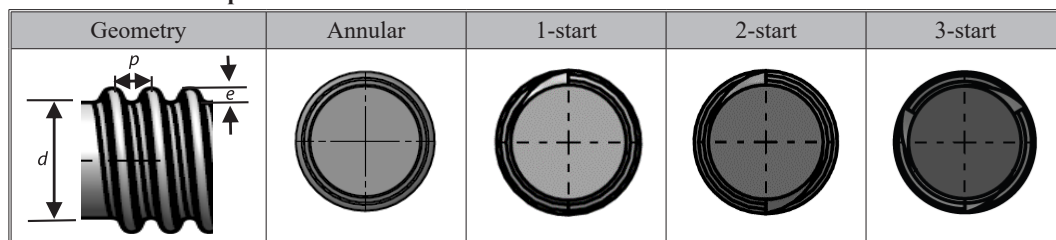


**Table 2. Geometrical parameters of the smooth tube and the flexible metal hoses**

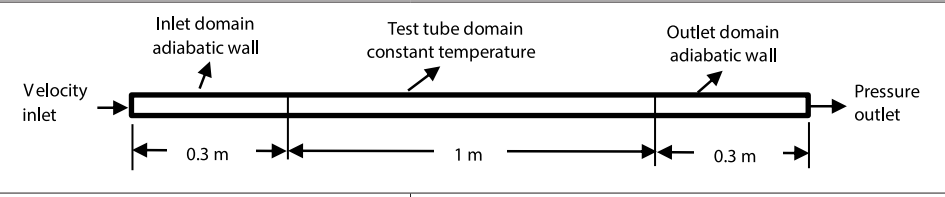
Geometry	$d_o$ [mm]	$d_i$ [mm]	$p$ [mm]	$d_h$ [mm]	$e$ [mm]	$A_s$ [m <sup>2</sup> ]
Smooth	–	25	–	25	–	0.079
Annular	30.65	24.2	5.4	25	3.2	0.153
1-start	32.65	26.2	5.8	26.2	3.2	0.151
2-start	32.65	26.2	11.6	26.2	3.2	0.152
3-start	32.65	26.2	17.7	26.2	3.2	0.152

The inner diameters of the 1-, 2-, and 3-start hoses were taken as hydraulic diameters. For comparison between the spiral corrugated hose and the annular corrugated hose, the geometric parameters of the annular corrugated hose were used as the reference.

### Numerical modelling

The test tube was modeled as a flexible stainless steel metal hose, 1 m in length, using the numerical domains and boundary conditions detailed in tab. 3. To ensure a fully developed turbulent flow, a smooth tube, approximately 0.3 meters in length (about 10 times the hydraulic diameter), was placed in front of the test tube. Additional smooth tubes at the inlet and outlet of the test tube were subjected to adiabatic wall boundary conditions.

**Table 3. Numerical domain and boundary conditions**

	
Operating parameters	Values
Inlet velocity	0.34-1.78 m/s
Inlet temperature	15 °C
Outlet pressure	0 Pa
Test tube surface temperature	70° C

The velocities were calculated for the Reynolds number range of 10000-50000, which served as the boundary condition *velocity inlet* at the tube inlet in tab. 3. The analysis was conducted with a fluid inlet temperature of 15 °C, a constant test tube surface temperature of 70 °C, and zero pressure at the outlet of the 0.3 m long smooth tube placed at the end of the test tube. As the numerical analyses were performed from the beginning of the 0.3 m long smooth tube, the diameter of the smooth tube was used as the characteristic length in the analyses. The analyses assumed an average water temperature of 25 °C. At this temperature, the thermo-physical properties of water were density  $\rho = 997 \text{ kg/m}^3$ , dynamic viscosity  $\mu = 0.891 \cdot 10^{-3} \text{ kg/ms}$ , specific heat  $c_p = 4180 \text{ kJ/kgK}$ , and thermal conduction coefficient  $k = 0.607 \text{ W/mK}$ , [18].

### Governing equations and numerical techniques

The ANSYS FLUENT (2022) was used to simulate the thermal-flow behavior of water in the smooth tube, annular corrugated hose, and spiral corrugated hoses via computational fluid dynamics. Under steady-state conditions, the following governing equations are for incompressible flows which have the three dimensions of continuity, momentum, and energy, respectively, Fluent Theory Guide, 2022 [19]:

$$\frac{\partial(\rho u_i)}{\partial x_i} = 0 \quad (1)$$

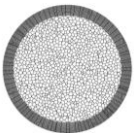
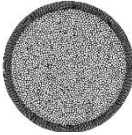
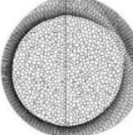
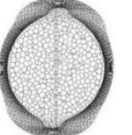

$$\frac{\partial(\rho u_i u_j)}{\partial x_j} = -\frac{\partial P}{\partial x_i} + \frac{\partial}{\partial x_j} \left[ \mu \left( \frac{\partial u_i}{\partial x_j} + \frac{\partial u_j}{\partial x_i} - \frac{2}{3} \delta_{ij} \frac{\partial u_k}{\partial x_k} \right) \right] + \frac{\partial}{\partial x_j} (-\rho \overline{u'_i u'_j}) \quad (2)$$

$$\frac{\partial}{\partial x_i} [u_i (\rho E + P)] = \frac{\partial}{\partial x_j} \left[ \left( k + \frac{c_p \mu_t}{\text{Pr}_t} \right) \frac{\partial T}{\partial x_j} + \mu u_i \left( \frac{\partial u_i}{\partial x_j} + \frac{\partial u_j}{\partial x_i} - \frac{2}{3} \delta_{ij} \frac{\partial u_k}{\partial x_k} \right) \right] \quad (3)$$

where  $E$  is the total energy,  $P$  – the static pressure,  $\mu_t$  – the turbulent viscosity,  $Pr_t$  – the turbulent Prandtl number, and  $k$  – the thermal conductivity.

We simulated the steady-state, incompressible 3-D water flow through both smooth and corrugated hoses with a constant wall temperature. A polyhedral mesh was chosen for this study, with a maximum skewness of 0.8 and a minimum orthogonal quality of 0.2. The semi-implicit method for pressure linked equations (SIMPE) algorithm was used for the solution. For the discretization of transport and governing equations, the second order upwind approach was adopted. The solutions were made with a  $y^+$  value of approximately 1. The SST  $k$ - $\omega$  turbulence model was preferred, and the PRESTO method was applied for pressure discretization. Details of the SST  $k$ - $\omega$  turbulence model can be found in [19]. Residual values for energy, and  $x$ -,  $y$ -, and  $z$ -momentum were set to  $10^{-5}$ . Examples of the solution mesh structures for each hose are shown in tab. 4.

**Table 4. Mesh structures**

Geometry	Smooth	Annular	1-start	2-start	3-start
Cross-section view					

#### Data reduction

The friction factor, logarithmic mean temperature difference, and convective heat transfer coefficients are defined [18, 20]:

$$f = \frac{2\Delta P d_h}{L\rho V^2} \quad (4)$$

$$\Delta T_{\ln} = \frac{T_i - T_{\text{out}}}{\ln \frac{T_s - T_{\text{out}}}{T_s - T_i}} \quad (5)$$

$$h = \frac{\dot{q}}{\Delta T_{\ln}} \quad (6)$$

The friction factor,  $f$ , was calculated by substituting the pressure drop results obtained from the numerical analysis of the smooth tube into eq. (4). The average fluid temperature at the outlet of the test tube ( $L = 1$  m) was considered to be the same as the temperature at the outlet of the 1.6 m long tube, because the analysis assumed adiabatic conditions for the 0.3 m long smooth tube surfaces placed at the inlet and outlet of the test tube, see tab. 3. The logarithmic mean temperature difference was determined using eq. (5) and then substituted into eq. (6). Additionally, the heat flux obtained from the analysis was substituted into eq. (6). Thus, the convective heat transfer coefficient,  $h$ , was derived from eq. (6). The Nusselt number was then calculated using the convective heat transfer coefficient. The relative differences between numerical results and correlations were calculated using eq. (7), [4]. The PEC is defined as the ratio of the heat transfer of an augmented surface to that of a smooth surface at equal pumping power [4]. In this study, the PEC for 1-, 2-, and 3-start spiral, and annular corrugated hoses compared to a smooth tube was calculated using eq. (8), [4]. The results of the analyses in the

smooth tube were presented in terms of both the friction factor,  $f_0$ , and Nusselt number,  $Nu_0$ , with a zero index:

$$\text{Relative difference} = \frac{(Nu_{\text{correlation}} - Nu_{\text{numeric}})100}{Nu_{\text{correlation}}} \quad (7)$$

$$\text{PEC} = \frac{Nu}{\left(\frac{f}{f_0}\right)^{1/3} Nu_0} \quad (8)$$

### Mesh independence

The pressure drop across the 1 m test tube, where the heat transfer occurred, was obtained from the pressure difference at the inlet and outlet in the simulations. Mesh independence studies were carried out by considering the fluid outlet temperature and pressure drop in the flows at the Reynolds number range of 10000-50000 for the smooth tube, annular corrugated hose, and 1-, 2-, and 3-start spiral corrugated hoses. For each hose, mesh independence studies were performed at  $Re = 1000-50000$  using three different mesh element numbers in general. As an example, the results of the mesh independence study for a corrugation depth of  $e = 3.2$  mm in each hose at  $Re = 10000$  are shown in tab. 5. We preferred using fewer mesh elements, as long as the results closely matched those from simulations with higher mesh elements.

**Table 5. Mesh independence test for  $e = 3.2$  mm at  $Re = 10000$**

Geometry	Smooth			Annular			1-start			2-start			3-start		
Number of mesh $\times 10^6$	3.8	4.87	5.95	6.5	8.36	9.55	8.2	9.2	10.76	6.2	8.7	9.7	7.87	9	10
$\Delta P$ [Pa]	77.4	77.5	77.8	264.1	262.6	261.7	207.4	208	207.5	224	219	220	213.5	214.4	214.2
$T_{\text{out}}$ [°C]	26.1	26.1	26	36.7	36.7	36.6	36.1	36.2	36.2	36.9	36	36	36.1	36.1	36.2

### Verification of numerical results

Two procedures were followed in the validation of the numerical studies:

- Experimental pressure drops were measured under adiabatic conditions and compared with the numerical analysis results under the same conditions.
- The results of the numerical analyses, taking heat transfer into consideration, were compared with the existing correlations in the literature in terms of both heat transfer and friction factor.

#### Experimental verification of pressure drop numerical results under adiabatic conditions

An experimental set-up was created for pressure drop measurements under the adiabatic flow conditions, as shown in fig. 1. All measuring instruments were properly calibrated. The differential pressure transducer measured the pressure drop with an accuracy of  $\pm 0.075\%$  FS (full scale) and the data logger transferred the data to a computer. The fluid-flow rate was

provided by an electromagnetic-flowmeter operating in the range of 0.4-4.5 m<sup>3</sup> per hour with a measurement error of ±0.5%. The temperature measurement error was about ±0.05 °C. As shown in tab. 3, 0.3 m smooth tubes were placed at the inlet and outlet of the 1 m test tube. The differential pressure transmitter – 3 measured the pressure difference at the inlet and outlet of this 1.6 m test section – 4. Under atmospheric conditions, the pump – 1 efficiently circulated water from the water tank – 6 to the test section – 4, and then returned it to the tank – 6. Flow rate values were determined based on the calculated fluid inlet velocities within the Reynolds number range of 20000-50000. Figure 2 shows photographs of the flexible metal hoses used in the pressure drop experiments. For the 1-start spiral hose, it was possible to perform the experiments with a corrugation depth of 2.1 mm instead of 3.2 mm as shown in tab. 6. We compared our experimental results with numerical simulations for the same hose geometry under adiabatic conditions, as shown in fig. 3. The pressure drop increased with increasing Reynolds numbers in all the three test tubes. With increasing Reynolds number, the difference between the experimental and numerical results increased for the annular corrugated hose, decreased for the 1-start spiral corrugated hose, and overlapped for the smooth tube. The maximum relative differences between the numerical and experimental results were 2.6%, 12.7%, and 11.8% for the smooth tube, annular corrugated hose, and 1-start spiral corrugated hose, respectively. For the smooth tube, the numerical results and the experimental pressure drops were within a narrow band of ±2.6%, as shown in fig. 4(a). Similar trends were observed for the annular corrugated and 1-start spiral corrugated hoses, with deviations within ±11% and ±13%, respectively, see figs. 4(b) and 4(c). These results validate the accuracy of the numerical model.

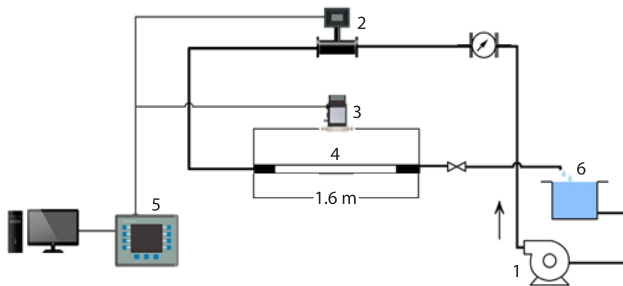


**Figure 1. Schematic representation of the experimental set-up:** 1 – water pump, 2 – flow meter, 3 – differential pressure transducer, 4 – test section, 5 – data logger, and 6 – water tank

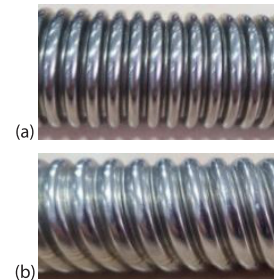


**Figure 2. Photographs of (a) annular corrugated hose and (b) 1-start spiral corrugated hose**

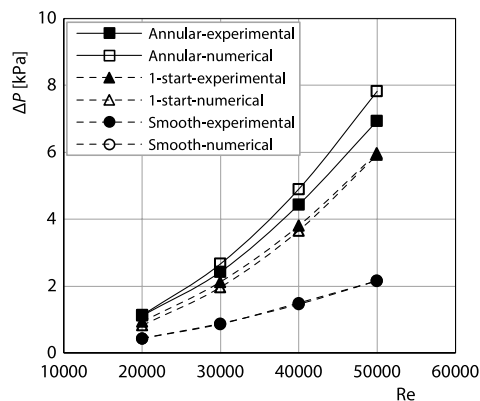


**Figure 3. Experimental and numerical results of the pressure drop**

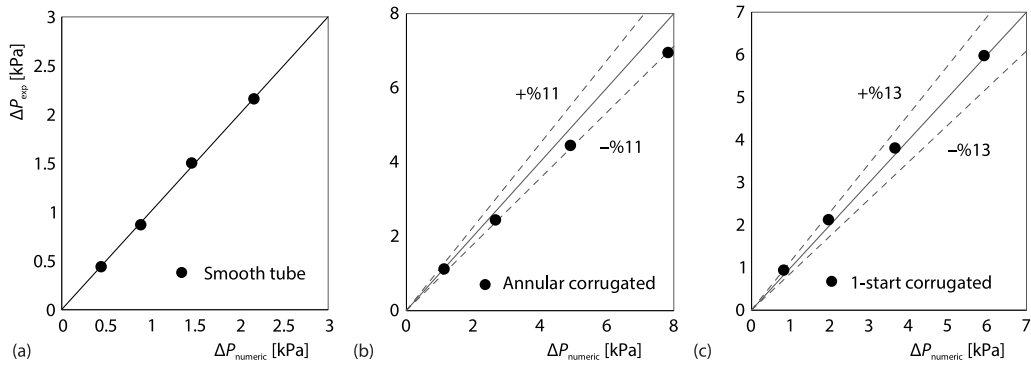


**Figure 4. Compatibility of experimental and numerical pressure drop results for; (a) the smooth tube, (b) annular corrugated hose, and (c) 1-start spiral corrugated hose**

**Table 6. Geometrical parameters of the test tubes for the experiments under adiabatic conditions**

Geometry	$d_o$ [mm]	$d_i$ [mm]	$p$ [mm]	$d_h$ [mm]	$e$ [mm]
Smooth	–	25	–	25	–
Annular	30.65	24.2	5.4	25	3.2
1-start	30.4	26.2	6.5	26.2	2.1

*Verification of the numerical results for the friction factors and the heat transfer with those of the correlations for smooth tubes*

The friction factors for the smooth tube were calculated using the correlations presented in tab. 7. As shown in fig. 5, both the friction factors obtained from the numerical analyses and those calculated using the existing correlations exhibit a decreasing trend with increasing Reynolds numbers. When compared with the correlation results, our numerical results showed relative differences of 1.3%-6.6% for the Haaland correlation, 3.5%-8.5% for the Blasius correlation, and 3.4%-8.3% for the Colburn correlation. There was good agreement between the friction factors obtained from the numerical analyses and those predicted using the well-known correlations, with a deviation band within  $\pm 10\%$ , see fig. 6.

**Table 7. Correlations for the friction factors existing in the literature**

Reference	Correlation	Validity range
[18]	$\frac{1}{\sqrt{f}} \cong -1.8 \log \left[ \frac{6.9}{Re} + \left( \frac{\varepsilon}{3.7d} \right)^{1.11} \right]$	$Re > 4000$
[18, 20]	$f = 0.184 Re^{-0.2}$	$Re \gg 20000$
[21]	$f = 0.3164 Re^{-1/4}$	$Re \leq 80000$

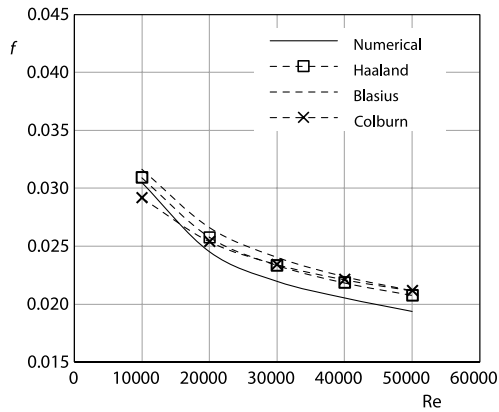


**Figure 5. Comparison of the numerical  $f$  values for the smooth tube with those of the correlations**

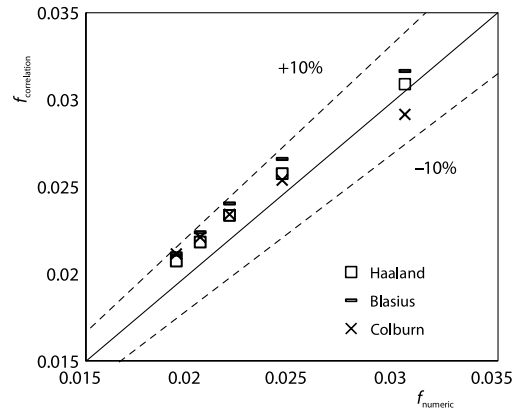


**Figure 6. The compatibility of the numerical  $f$  values with those of the ones obtained using the correlations**

To compare the results of the heat transfer analysis for the smooth tube, Nusselt number correlations for turbulent flow conditions in the existing literature were used, see tab. 8. Figure 7 shows the numerical Nusselt number results for the smooth tube compared with the results of the existing correlations. Both the analysis and correlation results showed that the Nusselt number increased with increasing Reynolds numbers. The relative differences of Nusselt numbers between the numerical results and the correlations were 0.1%-2.3% for the Sieder and Tate, 14.1%-18.9% for the Dittus Boelter, and 9.1%-26.5% for the Gnielinski. According to these results, the Sieder and Tate correlation showed the smallest relative differences. The Nusselt number results obtained from the numerical analyses show good agreement with the existing correlations within the  $\pm 16\%$  deviation bands, see fig. 8.

These results confirm the accuracy of both the friction factor and heat transfer analysis results for the smooth tube, as validated by the existing correlations in the literature.

**Table 8. Nusselt number correlations existing in the literature**

Reference	Correlation	Validity range
[18, 20]	$Nu = 0.023 Re^{4/5} Pr^{0.4}$	$0.7 \leq Pr \leq 120$ $2500 \leq Re \leq 1.24 \cdot 10^5$
[18, 20]	$Nu = 0.027 Re^{4/5} Pr^{1/3} (\mu/\mu_s)^{0.14}$	$0.7 < Pr < 16700$ $Re > 10^4$
[22]	$Nu = 0.0214(Re^{0.8} - 100)Pr^{0.4}$	$0.5 \leq Pr \leq 1.5$ $10^4 \leq Re \leq 5 \cdot 10^6$
	$Nu = 0.012(Re^{0.87} - 280)Pr^{0.4}$	$15 \leq Pr \leq 500$ $3 \cdot 10^3 \leq Re \leq 10^6$

## Results and discussion

This study numerically investigates how annular and spiral corrugation, along with the number of starts for spiral corrugation affect heat transfer and pressure drop in corrugated flexible metal hoses under turbulent flow conditions. Table 9 presents the velocity contours at radial cross-sections at the middle distance ( $L/2$ ) and velocity vectors at mid-planes parallel to the flow for  $Re = 40000$ ,  $e = 3.2$  mm, for 1-, 2-, and 3-start spiral corrugated hoses, and an

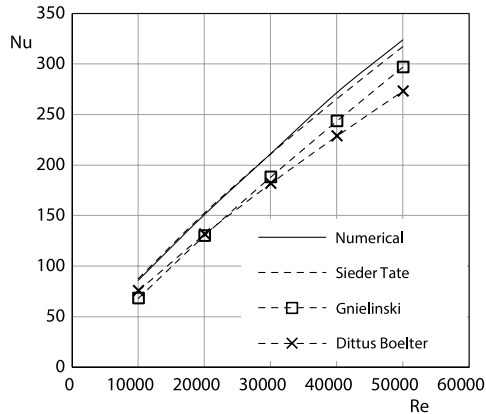


**Figure 7. Comparison of the numerical Nusselt number values for the smooth tube with those of the correlations**

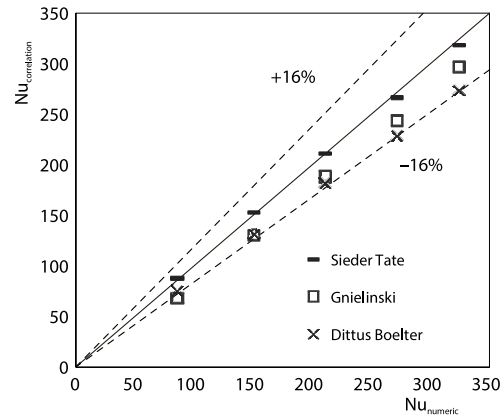
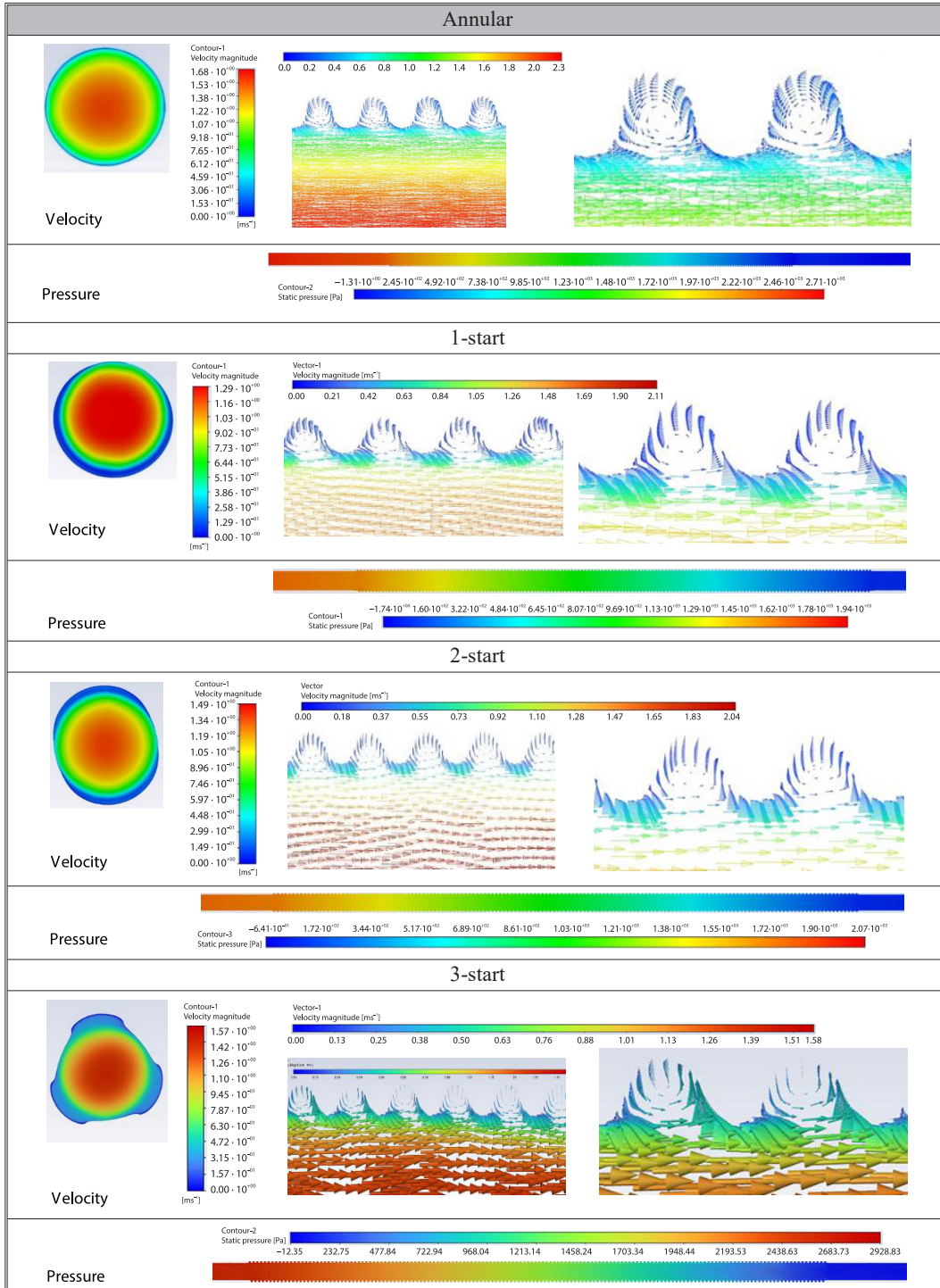


**Figure 8. The compatibility of the numerical Nusselt number values with those of the ones obtained using the correlations**

annular corrugated hose. The annular corrugated hose and spiral corrugated hoses with 1-start, 2-, and 3-starts form two groups of flow structures, one being the main vortex flow in the center and the other being the secondary vortex flow near the wall, as can be seen from the cross-sectional views in tab. 9. The velocity vectors at the mid-planes parallel to the flow show that secondary vortex flows are present in the corrugations of each flexible metal hose. The maximum axial velocity of the flow is observed in the center of all the flexible metal hoses. The velocity distributions in the radial direction vary depending on the start number of spiral corrugations. As previously reported in the [1], the number of secondary swirl flows also increases with an increase in the number of starts. Qian *et al.* [9] also report that the axial velocity increases with an increase in the number of starts in a spiral corrugated tube. Table 9 shows the pressure concentrating near the hose inlet, with a consistent decrease along the hose length for all hoses.

The analyses were carried out under constant temperature conditions at the surface of the hoses using water as the working fluid. The results are presented in comparison the smooth tube in terms of the friction factor ratio ( $f/f_0$ ), Nusselt number ratio ( $Nu/Nu_0$ ), PEC, fluid outlet temperature, and pressure drop. The friction factor ratio ( $f/f_0$ ) and Nusselt number ratio ( $Nu/Nu_0$ ) are obtained by dividing the numerical results for the friction factor and Nusselt number of the annular corrugated and the 1-, 2-, and 3-start spiral corrugated hoses by the numerical results for the smooth tube, where the smooth tube is denoted by a zero index. Figures 9(a)-9(c) show the variation of the friction factor ratios, Nusselt number ratios, and PEC values of the 1-, 2-, and 3-start spiral corrugated hoses and the annular corrugated hose with the Reynolds number, respectively. Figure 9(a) shows that the friction factor ratios increase with an increase in the Reynolds number. Al-dabagh *et al.* [16] identified several factors that simultaneously contribute to the increased pressure drop and the friction factor observed in corrugated tubes. These factors include drag forces exerted on the fluid-flow by the helical rib, rotational flow generated by the helical fin, increased frictional drag, and flow blockage related to the reduction of the tube's cross-sectional area. The combined effects of these factors with varied types of corrugation can result in higher pressure loss and an increased friction factor with an increased Reynolds number. From a Reynolds number of 10000-50000, the friction factor ratios of the 2- and 3-start spiral corrugated hoses are similar. Generally, the friction factor ratios of the 1-start spiral corrugated hose are higher than those of the others. In the Reynolds number range from 10000-20000, all corrugated hoses show similar friction factor ratios. At the Reynolds number

**Table 9. The velocity contours, velocity vectors, and pressure contours of the annular corrugated hose, and, 1-, 2-, and 3-start spiral corrugated hoses at  $Re = 40000$**



of 50000, the 1-start spiral corrugated hose has the highest friction ratio of 7.83, while the annular corrugated hose has the lowest at 6.23. As shown in fig. 9(a), the corrugated flexible metal hoses yield a friction factor in a range from 2.64-7.83 in comparison the smooth tube.

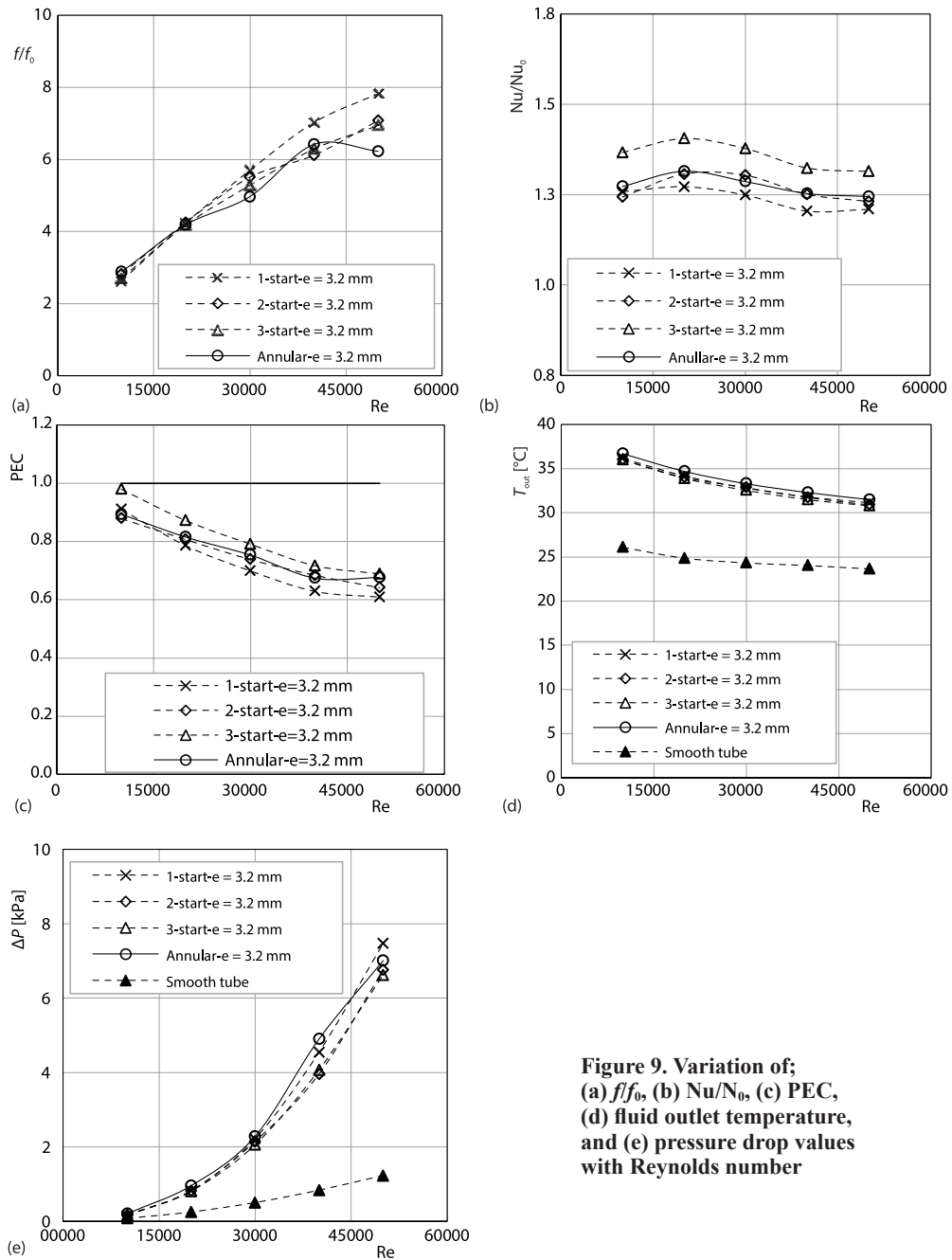


**Figure 9.** Variation of; (a)  $f/f_0$ , (b)  $Nu/Nu_0$ , (c) PEC, (d) fluid outlet temperature, and (e) pressure drop values with Reynolds number

Figure 9(b) shows that the Nusselt number increases for the corrugated hoses compared to that of the smooth tube. For spiral corrugation, the Nusselt number increases with an increase in the number of starts from 1-3, indicating improved heat transfer due to an increased swirl flow. According to Kongkai-paiboon *et al.* [1], an increase in the number of starts may result in stronger vortex intensity and thinning of the thermal boundary-layer on the tube surface, which facilitates heat transfer between the fluid and the tube walls. The Nusselt number ratios of the annular and 2-start spiral corrugated hoses are similar and fall between those of the 3- and 1-start spiral corrugated hoses. It is assumed that the 1-start spiral corrugation produces the weakest vortex flow, resulting in the weakest heat transfer. For the range studied, the Nusselt numbers of the corrugated hoses are 1.2-1.4 times higher than those of the smooth tube, with the maximum heat transfer observed for the 3- spiral corrugation at  $Re = 20000$ . The Nusselt number ratios for all hoses show a decreasing trend with increasing Reynolds numbers above 20000.

As shown in fig. 9(c), although the Nusselt numbers for all hoses are higher compared to those of the smooth tube, their PEC values range from 0.6-1 due to their high friction factor ratios. Among the hoses tested, the 3-start spiral corrugated hose provides the highest PEC, while the 1-start spiral corrugated hose, with the highest friction factor ratio, yields the lowest PEC. Consistent with previous research [1], the PEC generally decrease with increasing Reynolds numbers for all hoses. Figure 9(d) shows that the fluid outlet temperature values for the annular corrugated hose, the spiral corrugated hoses, and the smooth tube decrease with increasing Reynolds numbers. Of the corrugated hoses, the annular design provides the highest fluid outlet temperature for a given Reynolds number, followed by the 1-start spiral corrugated hose. The fluid outlet temperatures of the 2- and 3-start spiral corrugated hoses are similar, with difference in fluid outlet temperatures of the corrugated hoses generally being less than  $1\text{ }^{\circ}\text{C}$  for the same Reynolds number. Compared to the corrugated hose, the fluid outlet temperature of the smooth tube is  $11\text{ }^{\circ}\text{C}$  lower for  $Re = 10000$  and  $8\text{ }^{\circ}\text{C}$  lower for  $Re = 50000$ . Figure 9(e) shows the pressure drop for each hose and its variation with Reynolds number. The pressure drop increases with increasing Reynolds number for the annular corrugated hose, 1-, 2-, and 3-start spiral corrugated hoses, and the smooth tube. In fig. 9(e), it can be seen that the pressure drop for the 3-start corrugated hose is generally lower than that of the other hoses. Except for the pressure drop at  $Re = 50000$ , the pressure drop values of the annular corrugated hose are generally higher than those of the 1-, 2-, and 3-start spiral corrugated hose. At  $Re = 50000$ , the pressure drop of the 1-start corrugated hose is about six times higher than that of the smooth tube. The pressure drop of annular corrugated hose and 1-start spiral corrugated hose at  $Re = 40000$  is about 5.85 and 5.43 times higher than that of the smooth tube, respectively.

## Conclusions

The heat transfer and pressure drop in 1-, 2-, and 3-start spiral corrugated hoses, annular corrugated hose, and the smooth tube were numerically investigated. Annular and spiral corrugated hoses enhance heat transfer by promoting vortex flows that improve fluid mixing between the core and wall regions. However, this enhanced mixing also results in a higher pressure drop compared to that of the smooth tube. The results are presented as follows.

- In general, the friction factor values of the 1-start corrugated hose are higher than those of the other hoses. The 1-start corrugation yields a friction factor value, 7.83 times higher than that of the smooth tube at  $Re = 50000$ . Using corrugated hoses gives friction factor ratios ranging from 2.64-7.83.

- Spiral corrugated hoses show a trend of increasing Nusselt number ratios with an increasing number of starts. In particular, the 3-start spiral corrugation yields higher Nusselt number ratios than those of the other corrugations over the entire Reynolds number range studied, reaching a maximum Nusselt number ratio of 1.4 compared to that of the smooth tube at  $Re = 20000$ . The lowest Nusselt number ratios are observed for the 1-start spiral corrugated hose, while the Nusselt number ratios for the annular and 2-start corrugated hoses are similar. Overall, the Nusselt number ratios for the corrugated hoses range from 1.2-1.4.
- The PEC values for all hoses are in the range of 0.6-1. The PEC values for the 3-start spiral corrugated hose are higher than those of the other hoses.
- The fluid outlet temperature of the annular corrugated hose results in a higher temperature than that of the 1-, 2-, and 3-start spiral corrugated hoses. Among the spiral corrugated hoses, the 1-start corrugated hose has the highest fluid outlet temperature. In general, the difference between the fluid outlet temperatures of the corrugated hoses is less than  $1\text{ }^{\circ}\text{C}$  for the same Reynolds number. The maximum difference in the fluid outlet temperature between the smooth tube and corrugated hoses is  $11\text{ }^{\circ}\text{C}$ .
- In general, the pressure drop values of the 3-start spiral corrugated hose are lower than those of the other hoses, while the pressure drop values of the annular corrugated hose are higher than those of the spiral corrugated hoses. The pressure drop of the 1-start corrugated hose at  $Re = 50000$  is found to be about six times higher than that of the smooth tube.

This study demonstrates the potential of flexible metal hoses with annular and spiral corrugations, using geometries distinct from the ones used in previous research, as a method of enhancing heat transfer in heat exchangers. Therefore, the results are useful for heat exchanger applications. Nevertheless, further parametric studies are needed.

### Acknowledgment

The authors would like to thank the company AYVAZ for supporting the experimental research.

### Nomenclature

$A$  – area, [ $\text{m}^2$ ]  
 $d$  – tube diameter, [m]  
 $e$  – corrugation depth [mm]  
 $f$  – friction factor, [–]  
 $h$  – heat transfer coefficient, [ $\text{Wm}^{-2}\text{K}^{-1}$ ]  
 $k$  – thermal conductivity, [ $\text{Wm}^{-1}\text{K}^{-1}$ ]  
 $L$  – length of tube [m]  
 $Nu$  – Nusselt number ( $hd_h/k$ ), [–]  
 $p$  – pitch, [mm]  
 $Pr$  – Prandtl number, [–]  
 $\Delta P$  – pressure drop, [ $\text{Nm}^{-2}$ ]  
 $\dot{q}$  – heat flux [ $\text{Wm}^{-2}$ ]  
 $Re$  – Reynolds number ( $= Vd_h/\nu$ ), [–]  
 $T$  – temperature [ $^{\circ}\text{C}$ ]  
 $\Delta T_{\text{in}}$  – logarithmic mean temperature, [K]  
 $V$  – velocity [ $\text{ms}^{-1}$ ]

PEC – performance evaluation criteria, [–]

#### Greek symbols

$\varepsilon$  – roughness, [mm]  
 $\mu$  – dynamic viscosity, [ $\text{kgm}^{-1}\text{s}^{-1}$ ]  
 $\nu$  – kinematic viscosity, [ $\text{m}^2\text{s}^{-1}$ ]  
 $\rho$  – fluid density, [ $\text{kgm}^{-3}$ ]

#### Subscripts

h – hydraulic  
 i – inner, inlet  
 o – outer  
 out – outlet  
 s – surface  
 0 – related to smooth tube

### References

- [1] Kongkaitpaiboon, V., *et al.*, Effects of spiral start number and depth ratio of corrugated tube on flow and heat transfer characteristics in turbulent flow region, *J. Mechanical Science and Technology*, 33 (2019), 8, pp. 1-8

- [2] Kareem, Z. S., et al., Heat Transfer Enhancement in Two-Start Spirally Corrugated Tube, *Alexandria Engineering J.*, 54 (2015), 3, pp. 415-422
- [3] Sethumadhavan, R., Raja Rao, M., Turbulent Flow Friction and Heat Transfer Characteristics of Single- and Multi-Start Spirally Enhanced Tubes, *ASME J. Heat Transfer*, 108 (1986), 1, pp. 55-61
- [4] Haervig, J., et al., On the Fully-Developed Heat Transfer Enhancing Flow Field in Sinusoidally, Spirally Corrugated Tubes Using Computational Fluid Dynamics, *Int. J. Heat and Mass Transfer*, 106 (2017), Mar., pp. 1051-1062
- [5] Promthaisong, P., et al., 3-D Numerical Study on the Flow Topology and Heat Transfer Characteristics of Turbulent Forced Convection in Spirally Corrugated Tube, *Numerical Heat Transfer*, 69 (2016), Part A, pp. 607-629
- [6] Pethkool, S., et al., Turbulent Heat Transfer Enhancement in a Heat Exchanger Using Helically Corrugated Tube, *Int. Commun. Heat Mass Transfer*, 38 (2011), 3, pp. 340-347
- [7] Vicente, P. G., et al., Experimental Investigation on Heat Transfer and Frictional Characteristics of Spirally Corrugated Tubes in Turbulent Flow at Different Prandtl Numbers, *Int. J. Heat and Mass Transfer*, 47 (2004), 4, pp. 671-681
- [8] Dong, Y., et al., Pressure Drop Heat Transfer and Performance of Single-Phase Turbulent Flow in Spirally Corrugated Tubes, *Experimental Thermal Fluid Science*, 24 (2001), 3-4, pp. 131-138
- [9] Qian, J. Y., et al., Thermohydraulic Performance Evaluation of Multi-Start Spirally Corrugated Tubes, *Int. J. Heat and Mass Transfer*, 156 (2020), 119876
- [10] Jin, Z. J., et al., Effects of Pitch And Corrugation Depth On Heat Transfer Characteristics In Six-Start Spirally Corrugated Tube, *Int. J. Heat and Mass Transfer*, 108 (2017), Part A, pp. 1011-1025
- [11] Mimura, K., Isozaki, A., Heat Transfer And Pressure Drop Of Corrugated Tubes, *Desalination*, 22 (1977), 1-3, pp. 131-139
- [12] Al-Obaidi, A. R., Investigation on Effects of Varying Geometrical Configurations on Thermal-Hydraulics Flow in a 3-D Corrugated Pipe, *Int. J. Thermal Sciences*, 171 (2022), 107237
- [13] Al-Obaidi, A. R., et al., Analysis on Flow Structure and Improvement of Heat Transfer in 3-D Circular Tube with Varying Axial Groove Turbulator Configurations, *Heat Transfer*, 50 (2021), 7, pp. 7333-7348
- [14] Djordjevic, M. Lj., et al., Pressure Drop and Stability of Flow in Archimedean Spiral Tube with Transverse Corrugations, *Thermal Science*, 20 (2016), 2, pp. 579-591
- [15] Ponnusamy, S., et al., Experimental Studies on Heat Transfer and Friction Factor Characteristics of a Turbulent Flow for Internally Grooved Tubes, *Thermal Science*, 20 (2016), Suppl. 4, pp. S1005-S1015
- [16] Al-dabagh, A. M., et al., Effect of Corrugation Depth on Heat Transfer Enhancement and Flow Characteristics for Corrugated Tubes, *Journal of University of Babylon for Engineering Sciences*, 26 (2018), 7, pp. 164-181
- [17] Zhai, H., et al., The Influence of Corrugated Pipes Parameters on Heat Transfer Characteristics, *Thermal Science*, 28 (2024), 1A, pp. 257-267
- [18] Cengel, Y. A., *Heat and Mass Transfer: A Practical Approach*, McGraw-Hill, New York, USA, 2007
- [19] ANSYS Fluent Theory Guide, <http://www.ansys.com>, 2022
- [20] Incropera F., Dewitt, P. D., *Fundamentals of Heat and Mass Transfer*, Wiley, New York, USA, 1996
- [21] Blasius, P. R. H., Law of Similarity for Frictional Processes in Liquids (in German), *Forschungsheft*, 131 (1913), pp. 1-41
- [22] Gnielinski, V., New Equations For Heat And Mass Transfer In Turbulent Flow Pipes And Channels (in German), *Forschung im Ingenieurwesen A*, 41 (1975), 1, pp. 8-16